

Nanopore Logic Operation with DNA to RNA Transcription in a Droplet System

Masayuki Ohara,[†] Masahiro Takinoue,[‡] and Ryuji Kawano^{*,†}

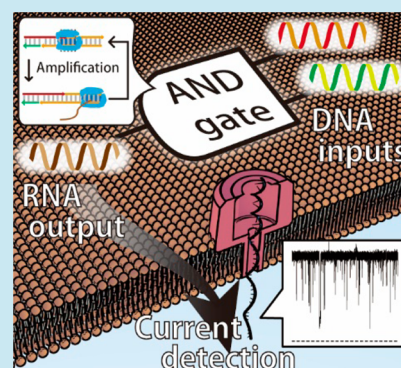
[†]Department of Biotechnology and Life Science, Tokyo University of Agriculture and Technology (TUAT), 2-24-16 Naka-cho, Koganei-shi, Tokyo 184-8588, Japan

[‡]Department of Computer Science, Tokyo Institute of Technology, 4259 Nagatsuta-cho, Yokohama, Kanagawa 226-8502, Japan

S Supporting Information

ABSTRACT: This paper describes an AND logic operation with amplification and transcription from DNA to RNA, using T7 RNA polymerase. All four operations, (0 0) to (1 1), with an enzyme reaction can be performed simultaneously, using four-droplet devices that are directly connected to a patch-clamp amplifier. The output RNA molecule is detected using a biological nanopore with single-molecule translocation. Channel current recordings can be obtained using the enzyme solution. The integration of DNA logic gates into electrochemical devices is necessary to obtain output information in a human-recognizable form. Our method will be useful for rapid and confined DNA computing applications, including the development of programmable diagnostic devices.

KEYWORDS: DNA computing, nanopore, lipid bilayer, droplet, microdevice



Nucleic acids have become important materials for the construction of programmable nanomaterials and medical systems in DNA computing.^{1,2} Initially, DNA computing based on logic operations was expected to outstrip electrical computing in terms of parallel processing ability. Recently, DNA computing has been applied to biological systems owing to its biocompatibility and programmability.³ Extensive studies have examined its applications to life systems, such as cellular circuits⁴ and medical diagnostics.⁵ With respect to diagnostics, mRNA and microRNA markers have been developed for the diagnosis of various cancers.^{6,7} Unlike typical diagnostic devices such as small glucose sensors, conventional DNA computing is operated in a nonintegrated system. In conventional logic operations, calculations are obtained by a three-step procedure, as follows: (1) DNA or RNA molecules are used as inputs in a solution and handled by pipetting, (2) enzyme reactions or chain displacement reactions occur in plastic tubes, and (3) output molecules and a human-recognizable readout are generated. To recognize output signals in conventional systems, multistep procedures such as fluorescent labeling, PCR (polymerase chain reaction), and gel electrophoresis are required. These procedures are not suitable for practical diagnostic applications.

We recently developed a method for the rapid and label-free detection of output DNA, using α -hemolysin (α HL) nanopores in microdroplet devices.⁸ DNA translocation through a nanopore can be detected electrically by the blocking of the channel current signal at the single-molecule level.^{9–11} Using this system, we previously constructed a NAND gate in a droplet device

that enables rapid detection (~ 10 min).⁸ However, this process has two issues. First, it is limited by the “one-to-one” reaction: the DNA hybridization or chain displacement reaction involves the same number of input and output molecules. The amplification of output molecules is imperative to construct a highly sensitive chip-based detection method. While PCR is broadly used for DNA amplification, it requires temperature cycling and accordingly, is not well suited for small chip operations. Another issue is that the input molecule and output molecule are of the same type; when DNA molecules are used as inputs, they are also the output in the system. The transcription function from DNA to RNA is useful for diagnosis or other medical applications, but it cannot be achieved in the conventional system.

To integrate amplification and transcription functions into the droplet system, we used a bacteriophage T7 RNA polymerase (T7RP) to construct a signal-amplified AND gate with DNA as the input and RNA as the output.¹² This amplification reaction can be performed in isothermal conditions and is suitable for integration into small chip operations. In this paper, we report that T7RP can be synthesized from input DNA to output RNA, using the AND operation, as shown in Figure 1. In addition, we were able to amplify the input DNA, resulting in a high concentration of output molecules; the output RNA molecules can be rapidly electrically detected using α HL nanopores.

Received: March 28, 2017

Published: April 17, 2017

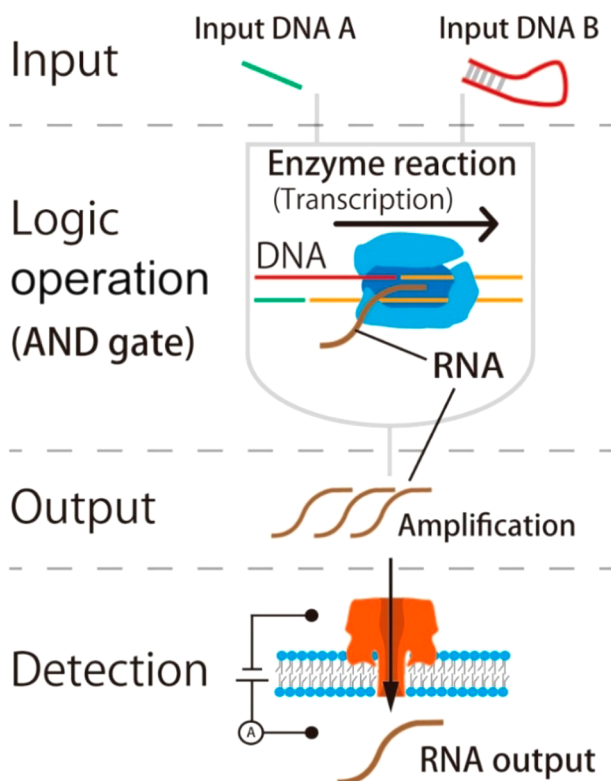


Figure 1. A schematic view of the AND gate with enzymatic reactions. When two types of inputs exist, RNA is synthesized by the T7 RNA polymerase. After RNA synthesis, these output molecules pass through α -hemolysin nanopores for detection.

The four individual calculations from (0 0) to (1 1) can be operated simultaneously using four-microdroplet devices.

RESULTS AND DISCUSSION

Principle of the AND Operation Using Biological Nanopores. To construct the AND gate with the reverse transcription enzyme, we used two input DNAs and template

DNAs containing part of the T7RP promoter region, as shown in Figure 2. For cases in which two input DNAs exist, defined as input (1 1), two input DNAs form a duplex and the duplex hybridizes with the template DNA. The T7RP polymerase binds to the promoter region and synthesizes a large amount of RNA as output 1 (Figure 2d). In other cases, inputs (0 0), (0 1), and (1 0), the input DNA cannot hybridize to the template DNA, resulting in output 0 (Figure 2a to 2c).

Design of the DNA for the AND Operation, Using a Thermodynamic Simulation. We designed the sequence of the input and template DNA molecules for the AND operation (Table 1) using a thermodynamic simulation. The design requisites were as follows: (i) the template DNA had the T7RP promoter region, which appeared only when both input DNAs exist at the same time, and (ii) one of the input DNAs did not bind to the promoter region of the template DNA in the (1 0) and (0 1) systems. The template DNA had a partial double-stranded region, although most of the T7RP promoter region remained single-stranded, as described in a previous report.¹² To ensure hybridization between the template and two input DNAs and a lack of hybridization for the single input DNA, we designed Input B such that it formed a hairpin structure; the double-stranded structure only formed in the presence of Input A. This dsDNA was able to bind to the template DNA and the enzyme reaction proceeded (Figure 2).

These DNAs were designed using thermodynamic simulations, and the base sequence and ΔG of each DNA system are listed in Tables 1 and 2. The ΔG of the hybridized structure of Inputs A and B was $-30.08 \text{ kJ mol}^{-1}$, indicating that the double-stranded structure was much more stable than the single-stranded structures (0 kJ mol^{-1}). The hybridized DNA could bind to the template DNAs to form the complete DNA structure containing Input A, Input B, and template DNAs. The calculated ΔG showed the largest stabilization energy, *i.e.*, $-99.66 \text{ kJ mol}^{-1}$, in this case. In contrast, when there was only one input DNA, template DNA binding did not occur based on the NUPACK simulation.

Verification of the AND Operation by Gel Electrophoresis. To confirm the AND operation using the designed

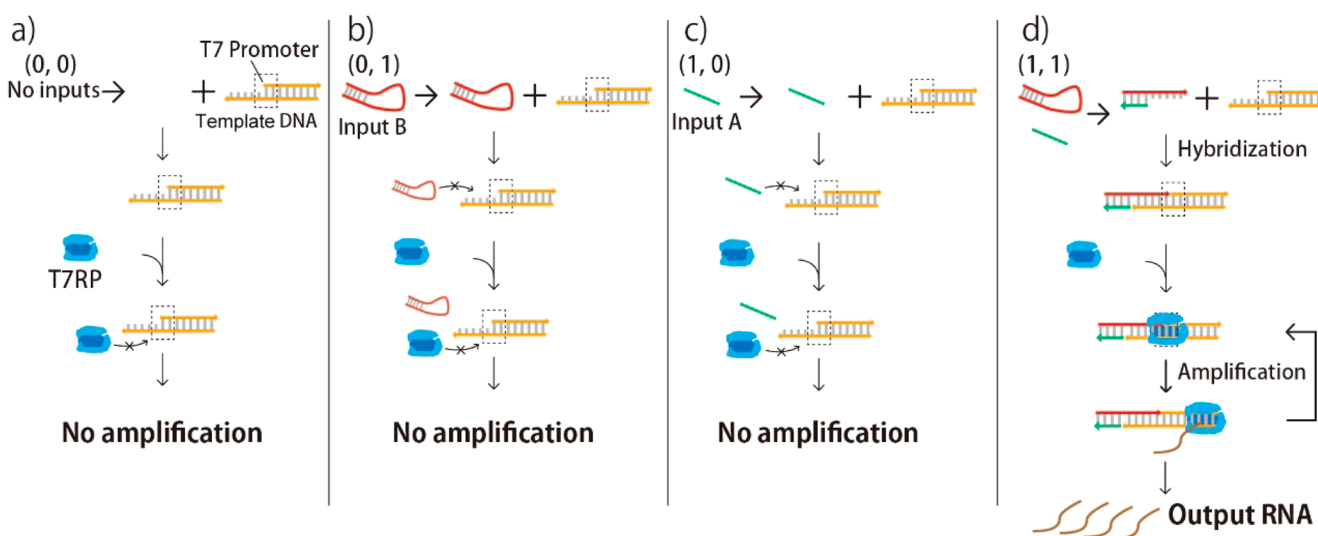


Figure 2. Reaction scheme for each input. (a–c) Output 0; Input DNA does not bind to the template DNA. Output RNA is not synthesized by T7RP because the enzyme cannot recognize the template DNA. (d) Output 1; Input DNA A and B can hybridize to each other. Subsequently, the input DNA binds to the template DNA. Finally, output RNA is synthesized by T7RP because the enzyme can recognize the input and template DNA complex.

Table 1. DNA Sequence for the AND Operation^a

Input DNA A	5'-CGAAGCAGCAGAAT CCGTAATA-3'	22 mer	Input DNA A	5'-CGAAGCAGCAGA- ATCCGTAATA-3'	22 mer	Input DNA A	5'-CGAAGCAGCAGA- ATCCGTAATA-3'
Input DNA B	5'-GTGAGTCGTATT ACGGATTCTGCT GCTTCGTAATACGACTCACTA-3'	45 mer	Input DNA B	5'-GTGAGTCGTATT- ACGGATTCTGCT TGCTTCGTAATACGAC- TCACTA-3'	45 mer	Input DNA B	5'-GTGAGTCGTATT- ACGGATTCTGCT GCTTCGTAATAC- GACTCACTA-3'

^aThe four individual calculations from (0 0) to (1 1) can be operated simultaneously using four-microdroplet devices.

Table 2. Gibbs Free Energy of DNA Combinations According to NUPACK Simulations

name	Input DNA A	Input DNA B	Input DNA A and B	temp. DNA 1	temp. DNA 2	temp. DNA 1 and 2	(1 1)
ΔG (kJ/mol)	0	-15.19	-30.08	-0.67	0	-44.58	-92.66

DNAs, we conducted the four calculations from input (0 0) to (1 1) in tubes, and the reaction results were examined by gel electrophoresis, as shown in Figure 3a. In the case of (1 1), a

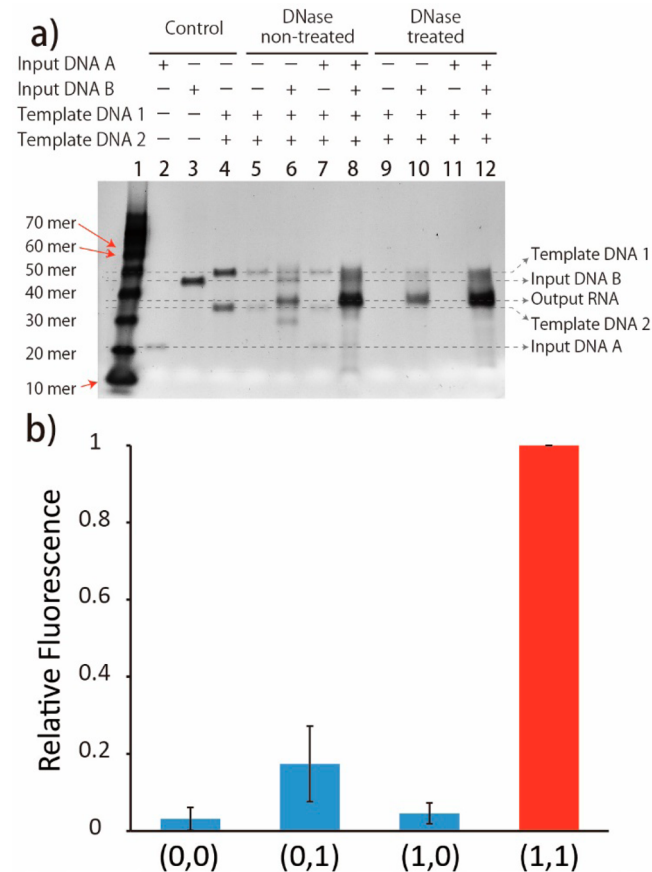


Figure 3. (a) Gel electrophoresis for the operation of RNA synthesis; 1 μ M each DNA with the control was applied in lanes 2, 3, and 4. (b) Relative fluorescence of output RNA without DNase. Error bars represent standard deviations ($n = 3$).

concentrated band was observed at around 35-mer DNA, comparable to the length of synthesized RNA. To verify RNA generation, we added DNase to degrade the DNAs. As a result, an unexpected band, consistent with RNA generation in the (0 1) system, was detected, suggesting that there were some errors. Although Input B formed a hairpin structure to prevent unexpected binding to the template DNA, this hairpin structure may dissociate, enabling the binding of the T7RP promoter region to the template DNA. As shown in Figure 3b, the (1 1)

system clearly exhibited the greatest RNA generation compared with other cases. In addition, this reaction differed between a conventional plastic tube and the droplet with a surrounding lipid layer (Figure S5). Therefore, we improved the droplet device by minimizing width to enhance heat transfer. We concluded that this system was sufficient for the AND operation by establishing an appropriate threshold (see Channel Current Measurements and Data Analysis).

Asymmetric Solution Conditions for Nanopore Measurement in a Two-Droplet System. We fabricated four-droplet contact devices to operate the four logic calculations simultaneously (Figure 4a). The devices can be dismantled from a breadboard, which was used as a platform for the electrical connection, and placed in a thermal cyclor during the enzyme reaction.¹³ To prevent droplet fusion and the mixture of the solutions before nanopore measurements, we prepared a separator that closes the aperture between each droplet chamber during the enzyme reaction (Figure 4b). In our two-droplet devices, one of the droplets was used as the logic operation (enzyme reaction) droplet and the other was the electrolyte solution, as shown in Figure 4c. Traditionally, nanopore measurements are performed using a symmetrical KCl solution to obtain appropriate channel current conductance. However, the enzyme activity of T7RP decreases in solutions with high KCl concentrations.¹⁴ Therefore, we used 0.2 M KCl for the enzyme solution. This concentration has two problems: a decreased the translocation event frequency¹⁵ and channel conductance. To address these problems, we used asymmetric electrolyte conditions (1 M KCl/0.2 M KCl).¹⁶ This asymmetric condition resulted in an 8-fold higher translocation frequency and 1.7-fold higher conductance than those of the symmetrical condition of (0.2 M KCl/0.2 M KCl).

AND Operation with Nanopore Measurements in Four Operation Devices. For the AND operation with nanopore measurements, the flowchart of the calculation protocol was configured as shown in Figure S2. (i) After nanopore opening, the blocking of current signals shorter than 500 ms and current blockage of less than 60% are measured for 5 s. (ii) Procedure (i) is repeated 3 times and the mean event frequency is determined. (iii) If the mean event frequency is larger than an established threshold value, the output is 1; otherwise, the output is 0.

Using this protocol, the AND logic operation was performed with the enzyme reaction and the output RNA was detected using nanopores. Figure 5a shows the typical current and time traces for all inputs, (0 0) to (1 1). In the case of (0 0), the blocking of current signals greater than 60% was not observed, but short current blocking events were detected. These short currents might indicate partial blocking events¹⁷ of template

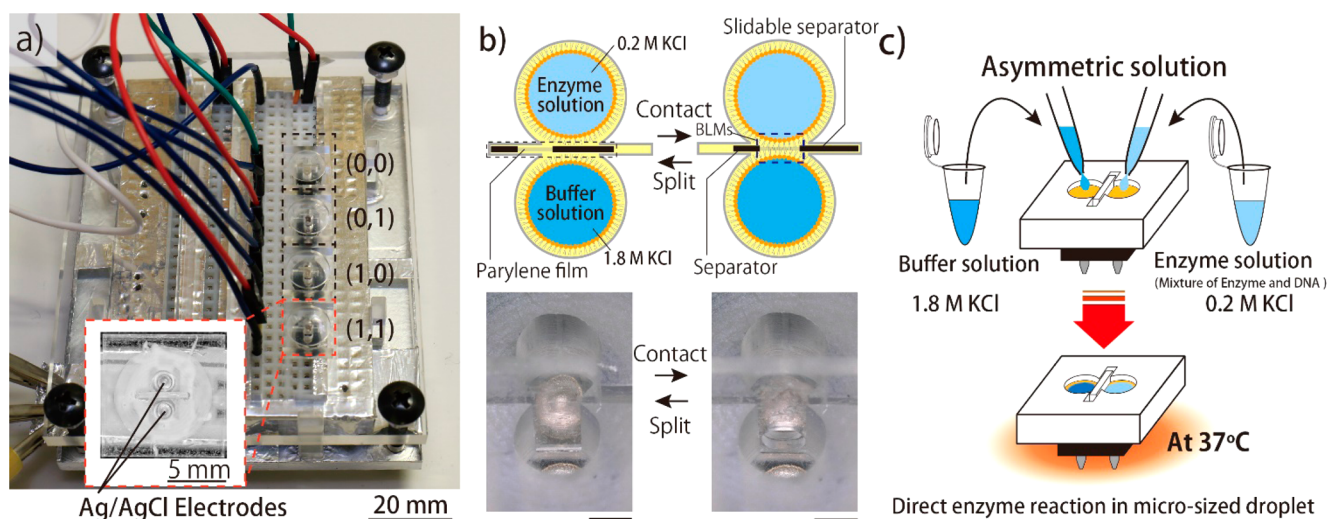


Figure 4. (a) The measurement system for electrical measurement. This system can measure each input solution simultaneously. (b) Image of the measurement multichannel device. Scale bar is 1 mm. (c) A schematic view of the experimental methods. Enzymatic reaction indicates activity for a droplet in the measurement device.

DNAs. In the cases of (1 0) and (0 1), large blocking signals were rarely observed, implying that unexpected RNA generation occurred, as mentioned above. In the case of (1 1), frequent blocking signals were observed. The mean event frequencies for each system are shown in Figure 5b. Setting the threshold to 0.702 s^{-1} based on the observed standard error and event frequency (see Channel Current Measurements and Data Analysis), we precisely defined the output signals in our droplet-nanopore system. All four-logic operations, (0 0) to (1 1), were carried out for 90 min, including 60 min of enzyme reaction. In addition, DNase can effectively reduce undesired translocation by the template or input DNAs (Figure S6). Combined with nanopore detection, the operation time can be much shorter than that of the conventional DNA logic operation (which can take several hours).^{18,19}

CONCLUSIONS

In summary, the signal-amplified AND operation with DNA-to-RNA transcription can be achieved using bacteriophage T7RP. Output RNA molecules were detected by α HL nanopores with the single-molecule translocation, and the system was label-free. The four different operations from (0 0) to (1 1) were successfully conducted simultaneously using the microdroplet devices. Using this method, the DNA/RNA transcription AND operation was performed over a short time period, using a time-consuming enzyme reaction. The enzyme reaction required *ca.* 60 min and was the rate-limiting process in the operation. To construct a rapid operation, other methods, such as toehold reactions, should be considered.

Highly complex operations, such as NAND or XOR with enzyme reactions, can be readily performed using our system. In addition, the integration of DNA logic gates into electrochemical devices is important to ensure that molecules containing output information, such as diagnostic results, can be processed as human-recognizable information.²⁰ In our system, the output molecules can be observed as nanopore current signals in microdroplet devices. This property is imperative for the practical usage in DNA computing, *e.g.*, microRNA²¹ or mRNA detection for cancer diagnosis.

METHODS

Reagents and Chemicals. The following reagents were used: 1,2-diphytanoyl-*sn*-glycero-3-phosphocholine (DPhPC; Avanti Polar Lipids, Alabaster, AL, USA), *n*-decane (Wako Pure Chemical Industries, Ltd., Osaka, Japan), Tris(hydroxymethyl)aminomethane (Tris; Nacalai Tesque, Kyoto, Japan), magnesium chloride (MgCl_2 ; Nacalai Tesque), potassium chloride (KCl; Nacalai Tesque), urea (Wako Pure Chemical Industries, Ltd.), Ribonucleoside Triphosphate mixture (NTP mixture, F. Hoffmann-La Roche, Ltd., Basel, Switzerland), 10 \times Transcription Buffer (500 mM sodium chloride, 80 mM magnesium chloride, 50 mM dithiothreitol, and 400 mM Tris-HCl, pH 8.0; TOYOBO Co., Ltd., Osaka, Japan), Thermo T7RP (TOYOBO), Ribonuclease inhibitor (RNase inhibitor, TOYOBO Co., Ltd.), deoxyribonuclease (DNase; Takara Bio, Inc., Shiga, Japan), ethylenediaminetetraacetic acid (EDTA; Nacalai Tesque), bromophenol blue (BPB, Wako), glycerol (Wako), Tris-Borate-EDTA buffer (TBE buffer; Takara Bio), ammonium persulfate (Wako), and 40% (w/v) Acrylamide/Bis Mixed Solution (Nacalai Tesque). Buffered electrolyte solutions were prepared from ultrapure water, which was obtained from a Milli-Q system (Millipore, Billerica, MA, USA). α HL (Sigma-Aldrich, St. Louis, MO, USA) was obtained as a monomer protein isolated from *Staphylococcus aureus* in the form of a powder, dissolved at a concentration of 1 mg/mL in ultrapure water, and stored at $-80 \text{ }^\circ\text{C}$. For use, samples were diluted to $0.3 \text{ } \mu\text{M}$ using a buffered electrolyte solution and stored at $4 \text{ }^\circ\text{C}$. This concentration was suitable for the single nanopore state, and the single pore cannot be perfectly controlled. Each DNA (FASMAC Co., Ltd., Kanagawa, Japan) was obtained from DNA synthesis in the form of a powder, dissolved at a concentration of $100 \text{ } \mu\text{M}$ in ultrapure water, and stored at $-20 \text{ }^\circ\text{C}$.

Design and Formation of Input and Template DNA. The free energy of Input DNA A, Input DNA B, and template DNA was calculated by thermodynamic simulations using Nucleic Acid Package (NUPACK) (<http://www.nupack.org/>).²² Annealing of the folded strands was conducted by heating each DNA sample for 5 min at $100 \text{ } \mu\text{M}$ in ultrapure water to $95 \text{ }^\circ\text{C}$, followed by rapid cooling to $4 \text{ }^\circ\text{C}$.

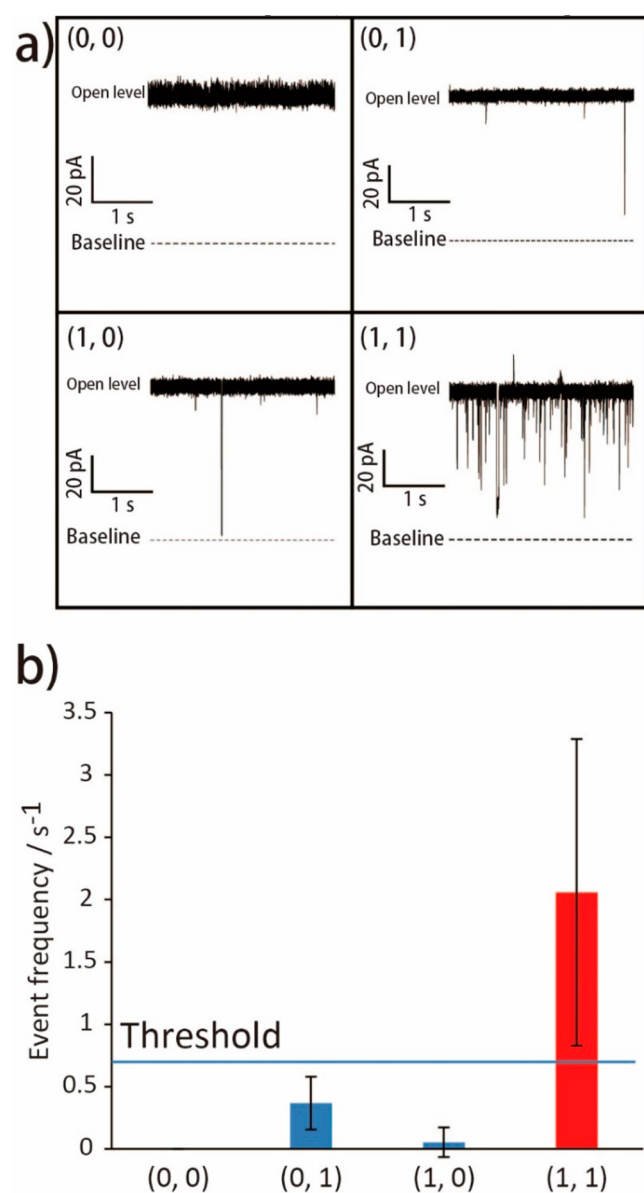


Figure 5. (a) Typical current traces of each input at +120 mV for 0.2 M KCl on the *trans* side, 1 M KCl on the *cis* side. (b) The event frequency for each input. Error bars indicate three times the standard error (3σ).

Preparation of the Multichannel Device. The multichannel device^{23,24} was fabricated by machining a 6.0 mm-thick, 10 × 10 mm poly(methyl methacrylate) (PMMA) plate (Mitsubishi Rayon, Tokyo, Japan), using computer-aided design and a computer-aided manufacturing three-dimensional modeling machine (MM-100; Modia Systems, Koshigaya, Japan), as shown in Figure 4a. Two wells (2.0 mm diameter and 5.0 mm depth) and a ditch between the wells were manufactured on the PMMA plate. Each well had a through-hole in the bottom and Ag/AgCl electrodes were set in the hole. A polymeric film made of parylene C (polychloro-*p*-xylylene) with a thickness of 5 μm was patterned with single pores (100 μm diameter) using conventional photolithography methods and then fixed between PMMA films (0.2 mm thick) using an adhesive bond (Super X; Cemedine Co., Ltd., Tokyo, Japan). The films, including the parylene film, were inserted into the ditch to separate the wells. Ag/AgCl electrodes of

each device were attached to a solderless breadboard (E-Call Enterprise Co., Ltd., Taipei City, Taiwan), which was connected to a Jet patch-clamp amplifier (Tecella, Foothill Ranch, CA, USA) using a jumper wire.

Gel Electrophoresis and Analysis of Fluorescence Intensity. Products of output RNA amplification were analyzed by 10% denaturing polyacrylamide gel electrophoresis (containing 19/1 acrylamide/bis (w/w)) in 1× TBE buffer (89 mM Tris-Borate, 2 mM EDTA, pH 8.3) at a 7.5 W constant power for 45 min at 22 ± 2 °C. The gel was made in our laboratory. After electrophoresis, the gel was stained with diluted SYBR Gold (Thermo Fisher Scientific, Waltham, MA, USA) solution for 30 min. Images were obtained under blue LED radiation using a digital camera. The fluorescent intensity was analyzed using ImageJ 1.50 (National Institutes of Health, Bethesda, MD, USA).

Enzymatic Reaction in Droplets, Preparation of Bilayer Lipid Membranes, and Reconstitution of α -Hemolysin. Bilayer lipid membranes (BLMs) were prepared using an arrayed device with four chambers on the breadboard. Four individual BLMs can be simultaneously formed in this device. First, the DPhPC (lipids/*n*-decane, 10 mg/mL) solution (2.3 μL) was added to all chambers. Next, the buffer solution (4.0 μL) without α HL, DNA, or proteins was poured into each recording chamber. The enzyme solution (4.7 μL) with α HL (final concentration 1 to 5 nM) and each DNA (final concentration 0.1 μM) was added to each ground chamber. In this study, the enzyme solution (200 mM KCl, 20 units of RNase inhibitor, 50 units of T7RP, 2 mM NTP mixture, 1× Transcription Buffer pH 8.0) was used for the ground chamber, and the buffer solution (1 M KCl, 1× Transcription Buffer pH 8.0) was used for the recording chamber. The devices were set in a thermal cycler during the enzyme reaction for 60 min at 37 °C. They were then mounted on a breadboard platform, and the separator was opened (Figure 4b). A few minutes after applying the sliding separator, the two lipid monolayers connected and formed BLMs, and α HL formed nanopores by reconstitution in the BLMs.

Channel Current Measurements and Data Analysis. Channel current was monitored using a Jet patch-clamp amplifier connected to each chamber. Ag/AgCl electrodes were already present in each droplet when the solution was added to the chambers. A constant voltage of +120 mV was applied to the recording chamber, and the ground chamber was grounded. Reconstituted α HL in BLMs allowed ions to pass through a nanopore under the voltage gradient, and channel current signals were obtained. When output RNA was present in the ground chamber, the RNA passed through the nanopore and channel current blockage was observed. Spike signals of RNA translocation were obtained, and the processes of electric current change were defined as a translocating event. When the BLMs ruptured, BLMs were reformed with the separator gate using tweezers. The signals were detected using a 4 kHz low-pass filter at a sampling frequency of 20 kHz. Analyses of channel current signals and duration were performed using pCLAMP ver. 10.6 (Molecular Devices, Sunnyvale, CA, USA) and Excel2013 (Microsoft, Redmond, WA, USA). RNA translocation events were obtained from more than 60% of the current blockades from an open current level in a single nanopore. Channel current measurements were conducted at 22 ± 2 °C. The detailed protocol of the AND operation described in Figure S2 as the flowchart. All operations were conducted from 5 to 16 times ($5 < n < 16$) in the nanopore

experiments. The threshold output for our AND gate was defined as follows:

$$y = \max\{\bar{x}_{(0,0)} + 3\sigma_{(0,0)}, \bar{x}_{(0,1)} + 3\sigma_{(0,1)}, \bar{x}_{(1,0)} + 3\sigma_{(1,0)}\} \quad (1)$$

$$z = \frac{\bar{x}_{(1,1)} - 3\sigma_{(1,1)} + y}{2} \quad (2)$$

where x indicates the event frequency, y is a maximum of three values, and z is the threshold value.

(i) The mean event frequency of three inputs (0 0), (1 0), and (1 1) and three times the standard error (3σ) were calculated. Each mean value and 3σ was added. The largest value of the three input patterns was determined. (ii) The mean event frequency of input (1 1) was determined by 3σ . (iii) The mean value of (i) plus (ii) was defined as the threshold.

■ ASSOCIATED CONTENT

📄 Supporting Information

The Supporting Information is available free of charge on the ACS Publications website at DOI: [10.1021/acssynbio.7b00101](https://doi.org/10.1021/acssynbio.7b00101).

Experimental details of the enzyme reaction and the protocol of logic operation (PDF)

■ AUTHOR INFORMATION

Corresponding Author

*E-mail: rjkawano@cc.tuat.ac.jp.

ORCID

Ryuji Kawano: [0000-0001-6523-0649](https://orcid.org/0000-0001-6523-0649)

Author Contributions

R. K. and M. T. conceived the original idea. M. O. conducted the experiments and M. O. and R. K. wrote the paper.

Notes

The authors declare no competing financial interest.

■ ACKNOWLEDGMENTS

This work was partially supported by KAKENHI (Molecular robotics: Nos. 24104002, 15H00803, and 16H06043) from MEXT Japan.

■ REFERENCES

- (1) Seeman, N. C. (2010) Nanomaterials based on DNA. *Annu. Rev. Biochem.* 79, 65–87.
- (2) Simmel, F. C., and Dittmer, W. U. (2005) DNA nanodevices. *Small* 1, 284–299.
- (3) Benenson, Y. (2009) Biocomputers: from test tubes to live cells. *Mol. BioSyst.* 5, 675–685.
- (4) Benenson, Y. (2012) Biomolecular computing systems: principles, progress and potential. *Nat. Rev. Genet.* 13, 455–468.
- (5) Jung, C., and Ellington, A. D. (2014) Diagnostic applications of nucleic acid circuits. *Acc. Chem. Res.* 47, 1825–1835.
- (6) Benenson, Y., Paz-Elizur, T., Adar, R., Keinan, E., Livneh, Z., and Shapiro, E. (2001) Programmable and autonomous computing machine made of biomolecules. *Nature* 414, 430–434.
- (7) Zhang, X. Y., Wang, Y., Fricke, B. L., and Gu, L. Q. (2014) Programming nanopore ion flow for encoded multiplex microRNA detection. *ACS Nano* 8, 3444–3450.
- (8) Yasuga, H., Kawano, R., Takinoue, M., Tsuji, Y., Osaki, T., Kamiya, K., Miki, N., and Takeuchi, S. (2016) Logic gate operation by DNA translocation through biological nanopores. *PLoS One* 11, e0149667.
- (9) Reiner, J. E., Balijepalli, A., Robertson, J. W. F., Campbell, J., Suehle, J., and Kasianowicz, J. J. (2012) Disease detection and

management via single nanopore-based sensors. *Chem. Rev.* 112, 6431–6451.

(10) Deamer, D. W., and Branton, D. (2002) Characterization of nucleic acids by nanopore analysis. *Acc. Chem. Res.* 35, 817–825.

(11) Branton, D., Deamer, D. W., Marziali, A., Bayley, H., Benner, S. A., Butler, T., Di Ventra, M., Garaj, S., Hibbs, A., Huang, X. H., Jovanovich, S. B., Krstic, P. S., Lindsay, S., Ling, X. S. S., Mastrangelo, C. H., Meller, A., Oliver, J. S., Pershin, Y. V., Ramsey, J. M., Riehn, R., Soni, G. V., Tabard-Cossa, V., Wanunu, M., Wiggin, M., and Schloss, J. A. (2008) The potential and challenges of nanopore sequencing. *Nat. Biotechnol.* 26, 1146–1153.

(12) Ayukawa, S., Takinoue, M., and Kiga, D. (2011) RTRACS: A Modularized RNA-dependent RNA transcription system with high programmability. *Acc. Chem. Res.* 44, 1369–1379.

(13) Ohara, M., Sekiya, Y., and Kawano, R. (2016) Hairpin DNA unzipping analysis using a biological nanopore array. *Electrochemistry* 84, 338–341.

(14) Matsukage, A. (1972) Effects of KCl concentration on transcription by E.coli RNA-polymerase I. Specific effect of combination of nucleoside triphosphates. *Mol. Genet.* 118, 11–22.

(15) Jeon, B. J., and Muthukumar, M. (2014) Polymer capture by alpha-hemolysin pore upon salt concentration gradient. *J. Chem. Phys.* 140, 015101.

(16) Wanunu, M., Morrison, W., Rabin, Y., Grosberg, A. Y., and Meller, A. (2010) Electrostatic focusing of unlabelled DNA into nanoscale pores using a salt gradient. *Nat. Nanotechnol.* 5, 160–165.

(17) Akeson, M., Branton, D., Kasianowicz, J. J., Brandin, E., and Deamer, D. W. (1999) Microsecond time-scale discrimination among polycytidylic acid, polyadenylic acid, and polyuridylic acid as homopolymers or as segments within single RNA molecules. *Biophys. J.* 77, 3227–3233.

(18) Li, W., Zhang, F., Yan, H., and Liu, Y. (2016) DNA based arithmetic function: a half adder based on DNA strand displacement. *Nanoscale* 8, 3775–3784.

(19) Seelig, G., Soloveichik, D., Zhang, D. Y., and Winfree, E. (2006) Enzyme-free nucleic acid logic circuits. *Science* 314, 1585–1588.

(20) Feng, L. Y., Lyu, Z. Z., Offenhausser, A., and Mayer, D. (2015) Multi-level logic gate operation based on amplified aptasensor performance. *Angew. Chem., Int. Ed.* 54, 7693–7697.

(21) Hiratani, M., Ohara, M., and Kawano, R. (2017) Amplification and quantification of an antisense oligonucleotide from target microRNA using programmable DNA and a biological nanopore. *Anal. Chem.* 89 (4), 2312–2317.

(22) Zadeh, J. N., Steenberg, C. D., Bois, J. S., Wolfe, B. R., Pierce, M. B., Khan, A. R., Dirks, R. M., and Pierce, N. A. (2011) NUPACK: analysis and design of nucleic acid systems. *J. Comput. Chem.* 32, 170–173.

(23) Kawano, R., Tsuji, Y., Sato, K., Osaki, T., Kamiya, K., Hirano, M., Ide, T., Miki, N., and Takeuchi, S. (2013) Automated parallel recordings of topologically identified single ion channels. *Sci. Rep.* 3, 1995.

(24) Watanabe, H., and Kawano, R. (2016) Channel current analysis for pore-forming properties of an antimicrobial peptide, magainin I, using the droplet contact method. *Anal. Sci.* 32, 57–60.